Planta (2012) 235:1209–1219
DOI 10.1007/s00425-011-1569-7

ORIGINAL ARTICLE

Ultrastructure of the innermost surface of differentiating normal and compression wood tracheids as revealed by field emission scanning electron microscopy

Jong Sik Kim · Tatsuya Awano · Arata Yoshinaga · Keiji Takabe

Received: 9 October 2011 / Accepted: 1 December 2011 / Published online: 16 December 2011

Abstract The ultrastructure of the innermost surface of *Cryptomeria japonica* differentiating normal wood (NW) and compression wood (CW) was comparatively investigated by field emission electron microscopy (FE-SEM) combined with enzymatic degradation of hemicelluloses. Cellulose microfibril (CMF) bundles were readily observed in NW tracheids in the early stage of secondary cell wall formation, but not in CW tracheids because of the heavy accumulation of amorphous materials composed mainly of galactans and lignin. This result suggests that the ultrastructural deposition of cell wall components in the tracheid cell wall differ between NW and CW from the early stage of secondary cell wall formation. Delignified NW and CW tracheids showed similar structural changes during differentiating stages after xylanase or β-mannanase treatment, whereas they exhibited clear differences in ultrastructure in mature stages. Although thin CMF bundles were exposed in both delignified mature NW and CW tracheids by xylanase treatment, ultrastructural changes following β-mannanase treatment were only observed in CW tracheids. CW tracheids also showed different degradation patterns between xylanase and β-mannanase. CMF bundles showed a smooth surface in delignified mature CW tracheids treated with xylanase, whereas they had an uneven surface in delignified mature CW tracheids treated with β-mannanase, indicating that the uneven surface of CMF bundles was related to xylans. The present results suggest that ultrastructural deposition and organization of lignin and hemicelluloses in CW tracheids may differ from those of NW tracheids.

Keywords Cellulose microfibril · Compression wood · *Cryptomeria japonica* · FE-SEM · Hemicellulose · Lignin

Abbreviations

CMF	Cellulose microfibril
CW	Compression wood
NW	Normal wood

Introduction

The wood cell wall is composed of various components with variations in the concentration between components. Each component is successively deposited and then forms a highly complex and dynamic three-dimensional cell wall organization (Terashima et al. 2009). The organization of wood cell wall components varies between species and cell types and is strongly related to variation in wood cell wall structure. Although considerable progress has been made in understanding the basic organization and functions of wood cell wall components, many questions still remain regarding the variation in wood cell wall structure.

Compression wood (CW), formed on the lower part of stems and branches of leaning softwood, develops a unique tracheid structure on eccentrically growing xylem (Timell 1986). CW tracheids typically have rounded cell walls composed only of S_1 and S_2 layers, with a thick S_1 layer and helical cavities in the S_2 layer (Timell 1986). CW tracheids also show chemically different compositions and concentrations of cell wall components compared to those

J. S. Kim · T. Awano · A. Yoshinaga · K. Takabe
Laboratory of Tree Cell Biology, Graduate School of Agriculture, Kyoto University, Kyoto 606-8502, Japan

Present Address:
J. S. Kim (✉)
Wood Science, Department of Forest Products, Swedish University of Agricultural Sciences, P.O. Box 7008, 750 07 Uppsala, Sweden
e-mail: jong_sik71@hotmail.com

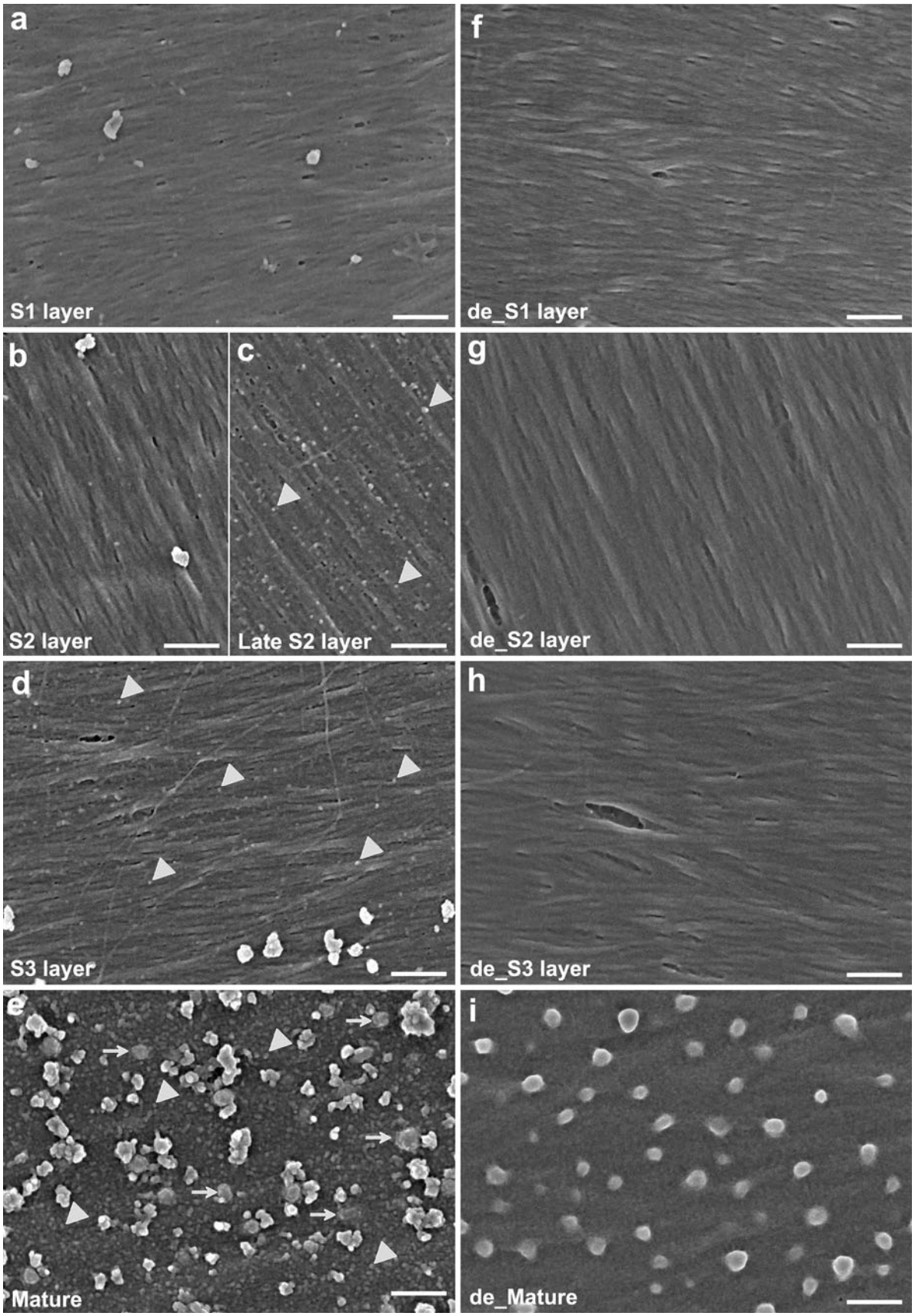
a
S1 layer
f
de_S1 layer
b
S2 layer
c
Late S2 layer
g
de_S2 layer
d
S3 layer
h
de_S3 layer
e
Mature
i
de_Mature

◀ **Fig. 1** The innermost surface of normal wood (NW) tracheids before (**a–e**) and after (**f–i**) delignification. **a–d**, **f–h** Differentiating tracheids. Cellulose microfibril (CMF) bundles were clearly observed in the innermost surface, particularly in the late S_2 and S_3 formation stages (**c**, **d**) with many globular substances (*arrowheads* in **c**, **d**). After delignification, CMF bundles were less likely to be visible compared to those before delignification in the late stages of secondary cell wall formation and globular substances on the CMF bundles were disappeared (**h**). **e**, **i** Mature tracheids. Many small globular structures (*arrowheads*) and warts (*arrows*) were observed in the warty layer (**e**), but small globular structures completely disappeared after delignification (**i**). Note no apparent CMF bundles on the surface after delignification (**i**). *Bar* 250 nm

of normal wood (NW) tracheids. CW tracheids contain more lignin, particularly in the outer S_2 layer, but less cellulose than NW tracheids (Donaldson 2001; Timell 1986). CW tracheids also contain more galactans (Nanayakkara et al. 2009; Timell 1986; Yeh et al. 2005, 2006) but fewer galactoglucomannans than NW tracheids (Côté et al. 1967; Hoffmann and Timell 1972; Timell 1986). In recent microscopic observations, Donaldson (2007) reported that the macrofibril diameter in the outer S_2 layer of CW tracheids is larger than that in NW tracheids and is correlated with chemical differences, mainly differences in lignin between NW and CW. However, the correlation between ultrastructure and CW tracheid cell wall components is poorly understood.

Hemicelluloses, the second largest class of polysaccharide in wood cell wall components, are generally considered as linked with cellulose and lignin to enhance the mechanical strength of the wood cell wall (Atalla 2005). Hemicelluloses are also considered as a controller that regulates the architecture of cell wall constituents (Atalla 2005). Several in vitro studies have shown that both mannans and xylans play an important role in the control of cellulose microfibril assembly (Iwata et al. 1998; Tokoh et al. 1998, 2002a, b; Uhlin et al. 1995). Several studies have also suggested that hemicelluloses function as templates for lignin deposition in the wood cell wall (Ruel et al. 2006; Salmén and Burgert 2009; Terashima et al. 2004, 2009). Our recent immunocytochemical studies determined that the distribution of hemicelluloses, particularly xylans and galactans in CW tracheids, differed significantly from that of NW tracheids (Kim et al. 2010, 2011). In combination with previous studies on functions of hemicelluloses as described above, our recent studies have suggested that hemicelluloses may be involved in the unique cell wall formation of CW tracheids in a way that differs from their involvement in the formation of NW tracheids (Kim et al. 2010, 2011). However, the relationship between hemicelluloses and CW tracheid ultrastructure is poorly understood.

To investigate differences in the organization of cell wall components between NW and CW tracheids, we investigated the ultrastructural properties of the innermost surface of differentiating NW and CW tracheid cell walls using field emission scanning electron microscopy (FE-SEM) in combination with specific hemicellulose enzyme degradation.

Materials and methods

Wood materials

Wood disks were sawn on 9 June 2009 from 32-year-old NW and on 18 May 2009 from 10-year-old artificial Japanese cedar (*Cryptomeria japonica*) CW grown at the Kyoto University Forest Station, Japan. Small blocks were collected from wood disks and stored in 70% ethanol before the FE-SEM observations.

Delignification with sodium chlorite

Delignification was performed according to previously described procedures (Kim et al. 2010) with minor modifications. Longitudinal sections (100 µm thick) of NW and CW were delignified with 8% $NaClO_2$ in 1.5% acetic acid at 40°C for 72 h and then washed several times with distilled water. Drying of samples was avoided during preparation to avoid alteration of structure.

Enzyme treatment

Longitudinal sections (100 µm thick) of NW and CW before and after delignification were incubated in 7.0 U xylanase (Sigma, USA) or 12.5 U β-mannanase (Megazyme, Ireland) in 0.1 M acetate buffer (pH 4.5) for 10 days at 35°C (Awano et al. 2002 with minor modifications). After several gentle washes with acetate buffer, some sections were continuously incubated in xylanase (if sections were initially treated with β-mannanase) or β-mannanase (if sections were initially treated with xylanase) using the same conditions described above for 1 week. As CW contains a high amount of galactans, some CW sections before and after delignification were also incubated for 10 days in 12.0 U endo-β-1,4-galactanase (Megazyme) in 0.1 M acetate buffer under the same conditions described above. All enzyme solutions were prepared fresh every 2 days. Some NW and CW sections before and after delignification were also incubated only with acetate buffer as a control. Drying of samples was avoided during preparation to avoid alteration of structure.

FE-SEM observations

All sections were post-fixed with 2% osmium tetroxide in 0.05 M phosphate buffer for 2 h at room temperature (Awano et al. 2002). Then they were dehydrated through a graded ethanol series, substituted with *t*-butyl alcohol and

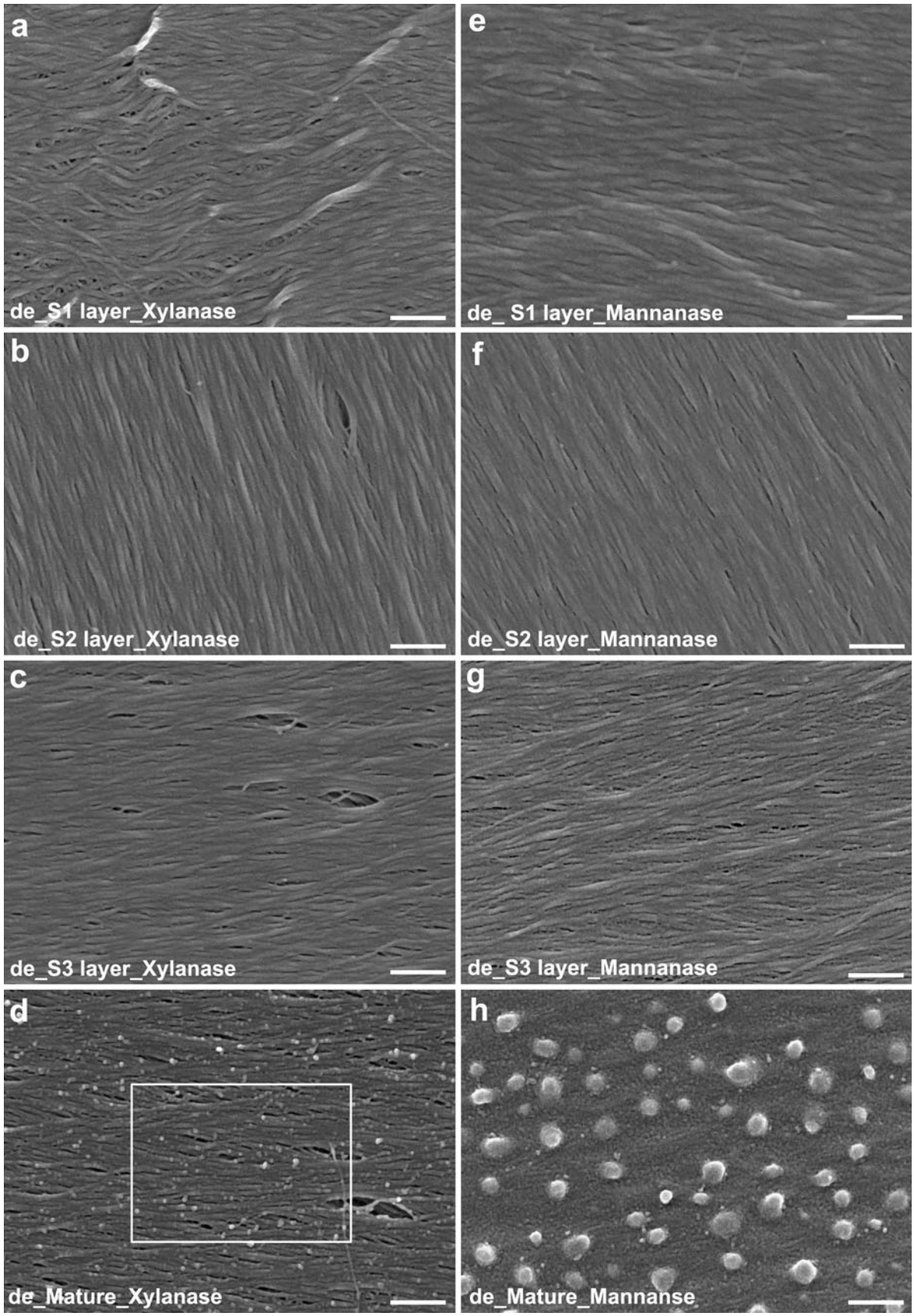
a
de_S1 layer_Xylanase
e
de_ S1 layer_Mannanase
b
de_S2 layer_Xylanase
f
de_S2 layer_Mannanase
c
de_S3 layer_Xylanase
g
de_S3 layer_Mannanase
d
de_Mature_Xylanase
h
de_Mature_Mannanse

◀ **Fig. 2** The innermost surface of delignified normal wood (NW) tracheids after xylanase (**a**–**d**) or *β*-mannanse (**e**–**h**) treatment. **a**–**c**, **e**–**g** Differentiating tracheids. Cellulose microfibril (CMF) bundles were more obvious after than before treatment (Fig. 1f–h) regardless of enzyme type. **d**, **h** Mature tracheids. Thin CMF bundles were observed on the surface with many small globular substances after xylanase treatment (**d**), but were not apparent after *β*-mannanse treatment (**h**). Note the almost intact wart structure after *β*-mannanse treatment compared to that before treatment (Fig. 1i) and some small globular substances on the surface (**h**). *Bar* 250 nm

freeze dried. Sections were coated with approximately 4–5 nm thick platinum with an ion sputter coater (E-1045; Hitachi, Tokyo, Japan) and examined under FE-SEM (S-4800; Hitachi) at an accelerating voltage of 1.5 kV and a 2.5 mm working distance.

Results

Ultrastructure of the innermost surface of NW tracheids before and after delignification

Figure 1 shows the innermost surface of differentiating NW tracheids before (a–e) and after (f–i) delignification. Cellulose microfibril (CMF) bundles were clearly observed in differentiating tracheids, particularly in the late S_2 and S_3 formation stages (Fig. 1c, d). CMF bundles were less likely to be visible after delignification than before delignification in late stages of secondary cell wall formation (Fig. 1g, h). Many globular substances were observed in tracheids during the late S_2 and S_3 stages (Fig. 1c, d), but disappeared after delignification (Fig. 1h).

CMF bundles were not apparent in mature tracheids regardless of delignification, due to masking by the warty layer (Fig. 1e, i). Warts and small globular structures were also observed in the warty layer (Fig. 1e). The small globular structures disappeared from this layer after delignification, whereas the warts remained (Fig. 1i).

Ultrastructure of the innermost surface of NW tracheids after hemicellulase treatment

NW tracheids before delignification showed no significant changes in ultrastructure after xylanase or *β*-mannanase treatment (data not shown). Controls incubated only in acetate buffer also did not show notable changes in ultrastructure regardless of delignification (data not shown). Notable changes in ultrastructure following enzyme treatments were only observed in delignified tracheids (Fig. 2). After xylanase (Fig. 2a–c) or *β*-mannanase (Fig. 2e–g) treatment, the finer structure of CMF bundles in delignified differentiating tracheids was visible compared to those before enzymatic treatment (Fig. 1f–h). However, ultrastructural differences were not clearly recognized between tracheids treated with either xylanase or *β*-mannanase during differentiating stages.

CMF bundles of the S_3 layer in delignified mature tracheids clearly appeared following xylanase treatment (Figs. 2d, 3), whereas they were not exposed by the *β*-mannanase treatment (Fig. 2h). Xylanase completely degraded the warty layer and warts in the delignified mature tracheids (Figs. 2d, 3), whereas *β*-mannanase did not significantly affect the warty layer structure or the warts (Fig. 2h). Many globular substances were also observed on CMF bundles in delignified mature tracheids after enzyme treatment (Fig. 3). The appearance of these substances differed from the globular substances observed in untreated differentiating NW tracheids (Fig. 1c, d).

Ultrastructure of the innermost surface of CW tracheids before and after delignification

CMF bundles were not readily observed on the innermost surface of differentiating CW tracheids, particularly in the early stage of secondary cell wall formation (Fig. 4a–e). Many amorphous materials were observed during the early CW tracheid stage (Fig. 4a, b). After delignification, CMF bundles were clearly visualized because amorphous materials had disappeared (Fig. 4g, h). During helical cavity formation, many globular substances, which differed structurally from those in NW tracheids (Fig. 1c, d), decreased gradually and then the CMF bundles assembled compactly (Fig. 4c–e). The globular substances completely disappeared in CMF bundles after delignification (Fig. 4i).

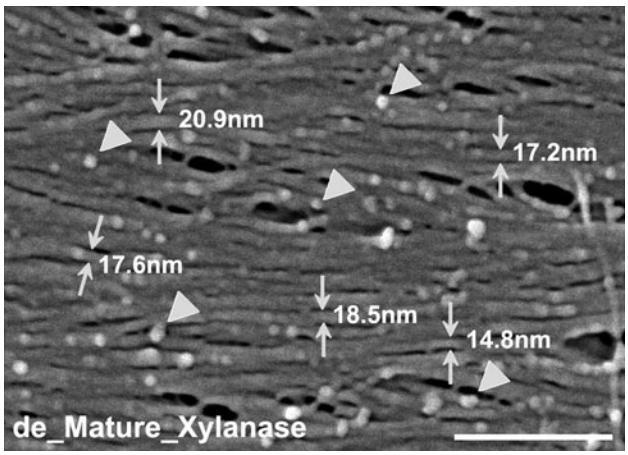

Fig. 3 The innermost surface of delignified mature normal wood (NW) tracheids after xylanase treatment. Enlargement of the square in Fig. 2d. The warts and the warty layer were completely removed and thin CMF bundles (*arrows*) were clearly observed on the surface. Note the many globular substances on the CMF bundles (*arrowheads*). Distance values between arrows indicate the thickness of CMF bundles. *Bar* 250 nm

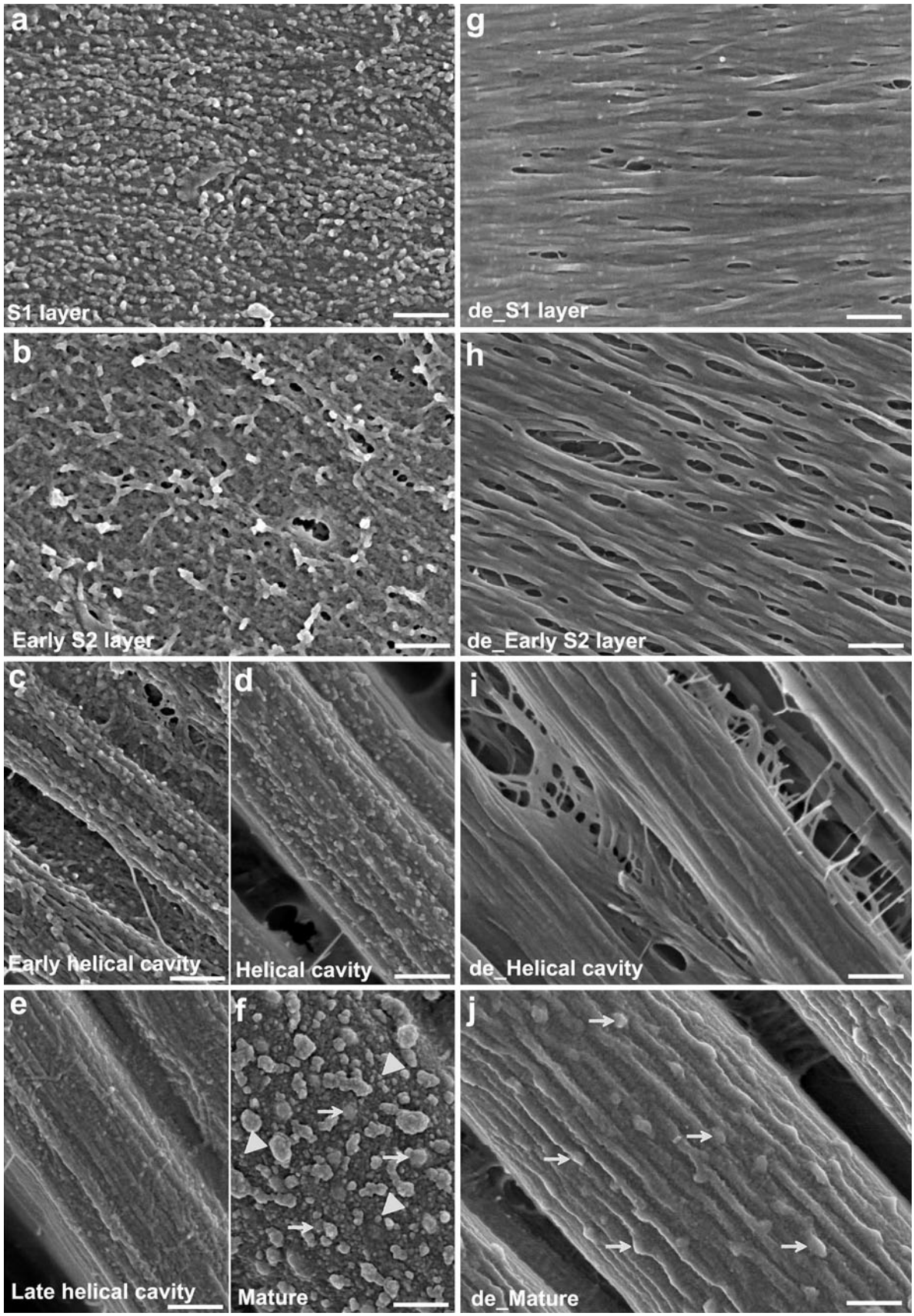
a
S1 layer
g
de_S1 layer
b
Early S2 layer
h
de_Early S2 layer
c
Early helical cavity
d
Helical cavity
i
de_Helical cavity
e
Late helical cavity
f
Mature
j
de_Mature

◀ **Fig. 4** The innermost surface of compression wood (CW) tracheids before (**a**–**f**) and after (**g**–**j**) delignification. **a–e**, **g–i** Differentiating tracheids. Cellulose microfibril (CMF) bundles were not clearly apparent in the early stages of secondary cell wall formation (**a**, **b**), but were clearly visualized after delignification because amorphous materials has disappeared (**g**, **h**). During helical cavity formation, globular substances decreased gradually and the CMF bundles were assembled more compactly (**c–e**). **f**, **j** Mature tracheid. Many small globular structures (*arrowheads*) and warts (*arrows*) were observed in the warty layer (**f**), but most small globular structures disappeared after delignification (**j**). Note the apparent CMF bundles on the surface after delignification (**j**). *Bar* 250 nm

CMF bundles were not apparent in mature tracheids due to masking by the warty layer (Fig. 4f), as in NW tracheids (Fig. 1e). Warts and numerous small globular structures were also observed in the warty layer (Fig. 4f). Unlike NW tracheids, thick CMF bundles were apparent with warts in delignified mature CW tracheids (Fig. 4j).

Ultrastructure of the innermost surface of CW tracheids after hemicellulase treatment

CW tracheids before delignification but after xylanase or β-mannanase treatment did not show notable ultrastructural changes compared to the control incubated only in acetate buffer (data not shown). As in the NW tracheids, delignified CW tracheids treated with xylanase (Fig. 5a–c) or β-mannanase (Fig. 5e–g) had a finer CMF bundle structure than those before the treatments (Fig. 4g–i). However, no significant differences were observed in the degradation patterns between the xylanase and β-mannanase treatments within differentiating stages.

In contrast to mature NW tracheids (Fig. 2h), delignified mature CW tracheids treated with β-mannanase showed notable ultrastructural changes of the innermost surface (Fig. 5h) and exhibited different degradation patterns than those treated with xylanase (Fig. 5d). Delignified mature tracheids treated with xylanase showed a smooth CMF bundle surface (Fig. 6a), whereas delignified mature tracheids treated with β-mannanase revealed an uneven CMF bundle surface (Fig. 6b) and thinner CMF bundle structures than those treated with xylanase (Fig. 6a). Delignified mature tracheids treated with β-mannanase, followed by xylanase treatment (Fig. 6c), had similar CMF bundle structures as those treated only with xylanase (Fig. 6a).

Unlike xylanase and β-mannanase, endo-β-1-4-galactanase induced some ultrastructural changes in differentiating CW tracheids before delignification (Fig. 7). In the early stage of secondary cell wall formation, particularly in the early S_2 stage, amorphous materials decreased significantly following endo-β-1-4-galactanase treatment (Fig. 7b, d), compared to controls (Fig. 7a, c). However, no significant ultrastructural changes were observed from the helical cavity formation stage to the mature stage compared to those in the control incubated only in acetate buffer (data not shown). Notable ultrastructural changes were also not clearly recognized in delignified mature tracheids treated with endo-β-1-4-galactanase compared to controls (data not shown).

Discussion

The wood cell wall maintains a complex organization pattern, and its structure differs among species and cell types. CW tracheids have different anatomical and chemical properties from NW tracheids. However, topochemical information about the CW tracheid cell wall is not well known. The present work demonstrates different ultrastructural organization of hemicelluloses and lignin between NW and CW tracheids. In this work, we do not exclude the possibilities of some alterations in chemical properties of the cell wall during sample preparations, particularly by delignification. However, previous study performed using a similar approach showed small differences in chemical properties of fibers between before and after delignification (Awano et al. 2002).

Our FE-SEM observations showed clear differences in cell wall formation between NW and CW tracheids. CMF bundles were clearly observed in NW tracheids in the early stages of secondary cell wall formation (Fig. 1a, b), whereas they were not observed in CW tracheids due to the heavy accumulation of amorphous materials (Fig. 4a, b). This result indicates that the process of CW tracheid cell wall formation may differ from that of NW tracheids in the early stage of secondary cell wall formation. It can also be expected that the amorphous materials may be involved in lignin accumulation, because they were only removed after delignification regardless of enzyme treatment. The heavy accumulation of amorphous materials in the cell wall at the early secondary cell wall formation also is spatially consistent with the high lignin concentration in the outer S_2 layer of CW tracheids (Donaldson 2001; Timell 1986). Amorphous materials were also partially degraded by endo-β-1-4-galactanase in CW tracheids in the early stage of S_2 formation, indicating that some of the amorphous material may be composed of galactans (Fig. 7). This result is consistent with our previous immunocytochemical study, in which most β-(1-4)-galactan labeling was present in the outer S_2 layer in differentiating CW tracheids of *Cryptomeria japonica* (Kim et al. 2010).

NW and CW showed structurally different types of substances on the CMF bundles during tracheid maturation. NW tracheids showed many globular substances on the

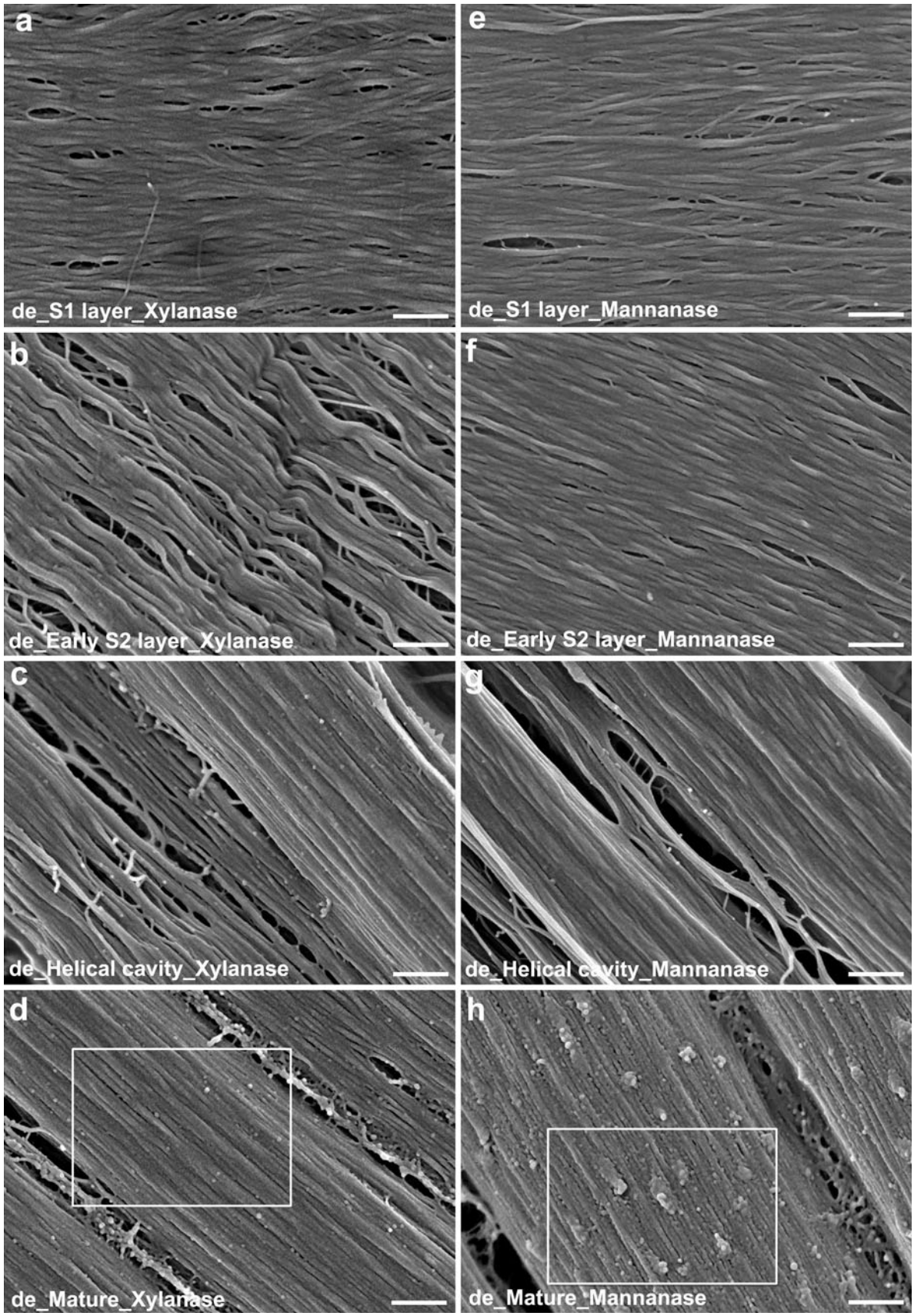
a
de_S1 layer_Xylanase
e
de_S1 layer_Mannanase
b
de_Early S2 layer_Xylanase
f
de_Early S2 layer_Mannanase
c
de_Helical cavity_Xylanase
g
de_Helical cavity_Mannanase
d
de_Mature_Xylanase
h
de_Mature_Mannanase

◀ **Fig. 5** The innermost surface of delignified compression wood (CW) tracheids after xylanase (**a**–**d**) or *β*-mannanse (**e**–**h**) treatment. **a**–**c**, **e**–**g** Differentiating tracheids. Cellulose microfibril (CMF) bundles were more obvious after than before treatment (Fig. 4g–i) regardless of enzyme type. **d**, **h** Mature tracheids. Warts degraded completely after xylanase treatment (**d**), whereas they remained after *β*-mannanse treatment (**h**). *Bar* 250 nm

CMF bundles in late stages of cell wall formation (Fig. 1c, d). CW tracheids also showed many globular substances on the CMF bundles during helical cavity formation (Fig. 4c, d), but their structural characteristics were different from those in NW tracheids. At present, we assume that they may have similar roles in cell wall formation related to lignin accumulation between CMF bundles in NW and CW tracheids. This assumption could be more clearly supported by changes in CMF bundles of CW tracheids. The globular substances decreased gradually during helical cavity formation, and the CMF bundles became compactly assembled, which may reflect cell wall lignification (Fig. 4c–e). Terashima et al. (2004, 2009) also suggested that the globular substances observed in the cell wall during tracheid formation may be lignin (lignin modules).

CMF bundles of NW and CW tracheids were not apparent in mature tracheids, because of masking by the warty layer, including warts and many small globular structures (Figs. 1e, 4f). CMF bundles did not appear in NW tracheids after delignification (Fig. 1i), whereas structures such as thick CMF bundles were apparent in CW tracheids (Fig. 4j), indicating that the chemical composition of the warty layer may differ between NW and CW tracheids. In addition, the small globular structures disappeared in the warty layer in both tracheids after delignification, whereas the warts remained (Figs. 1i, 4j). This result indicates that the small globular structures may be mostly composed of lignin, whereas the warts may be composed of lignin (Baird et al. 1974; Côté and Day 1962) with some other cell wall components such as xylans (Figs. 2d, 5d).

Both NW and CW showed a finer structure of the CMF bundles in delignified differentiating tracheids after hemicellulase treatment than before enzymatic treatment, which may reflect xylan or mannan degradation on the surface of the CMF bundles (Figs. 2a–c, e–g; 4a–c, e–g). However, no significant differences were observed in the ultrastructure between NW and CW tracheids following the enzyme treatments in the differentiating stages, even though our previous study showed significant differences in hemicellulose distribution between NW and CW, particularly xylans, in differentiating tracheids (Kim et al. 2011).

In contrast to the differentiating stages, delignified mature NW and CW tracheids showed significant differences in ultrastructural properties, particularly after *β*-mannanase treatment. NW tracheids were almost not affected after

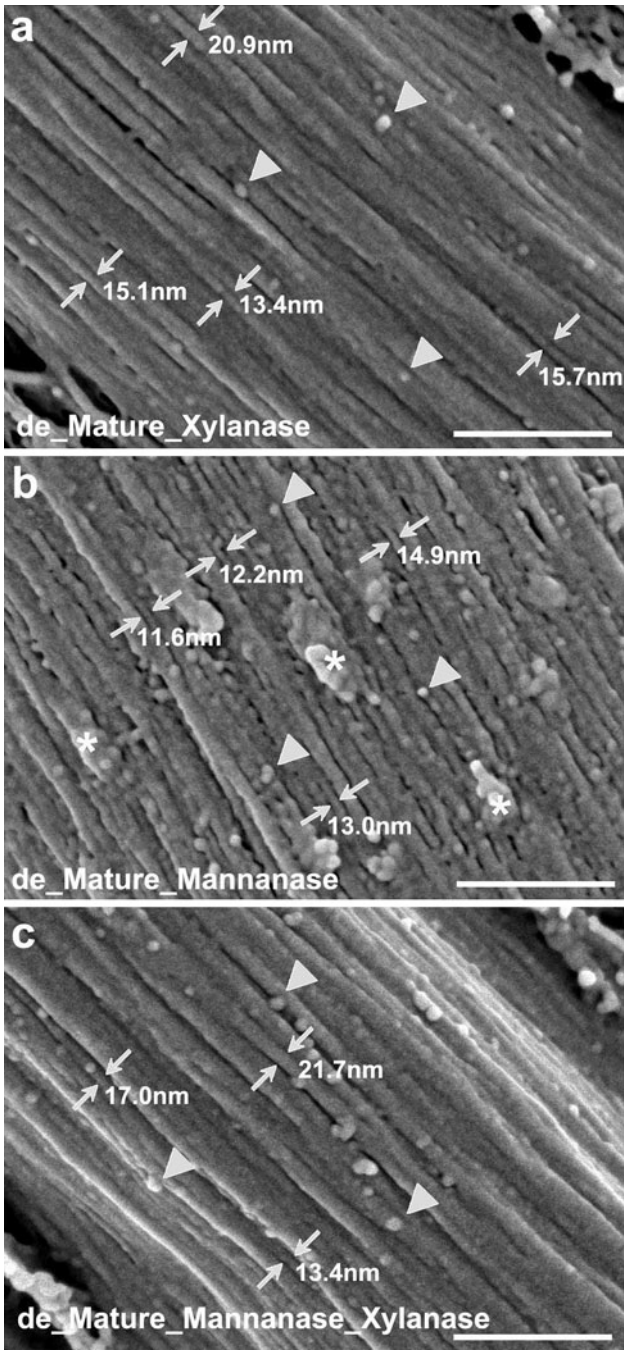

Fig. 6 The innermost surface of delignified mature compression wood (CW) tracheids after xylanase (**a** enlargement of the square in Fig. 5d), *β*-mannanse (**b** enlargement of the square in Fig. 5h), or *β*-mannanse treatment followed by xylanase (**c**) treatment. Tracheids treated with xylanase showed a smooth cellulose microfibril (CMF) bundle surface (**a**), whereas those treated with *β*-mannanse showed an uneven CMF bundle surface (**b**). Tracheids treated with xylanase (**a**) also showed thicker (*arrows* in **a**, **b**) and more compactly assembled CMF bundles than those treated with *β*-mannanse (**b**). A similar CMF bundle structure to those treated only by xylanase (**a**) was observed after *β*-mannanse treatment followed by xylanase treatment (**c**). Note the many globular substances (*arrowheads* in **a**–**c**) and completely (**a**, **c**) or partially degraded warts (*thick arrows* in **b**). Distance values between arrows indicate the thickness of CMF bundles. *Bar* 250 nm

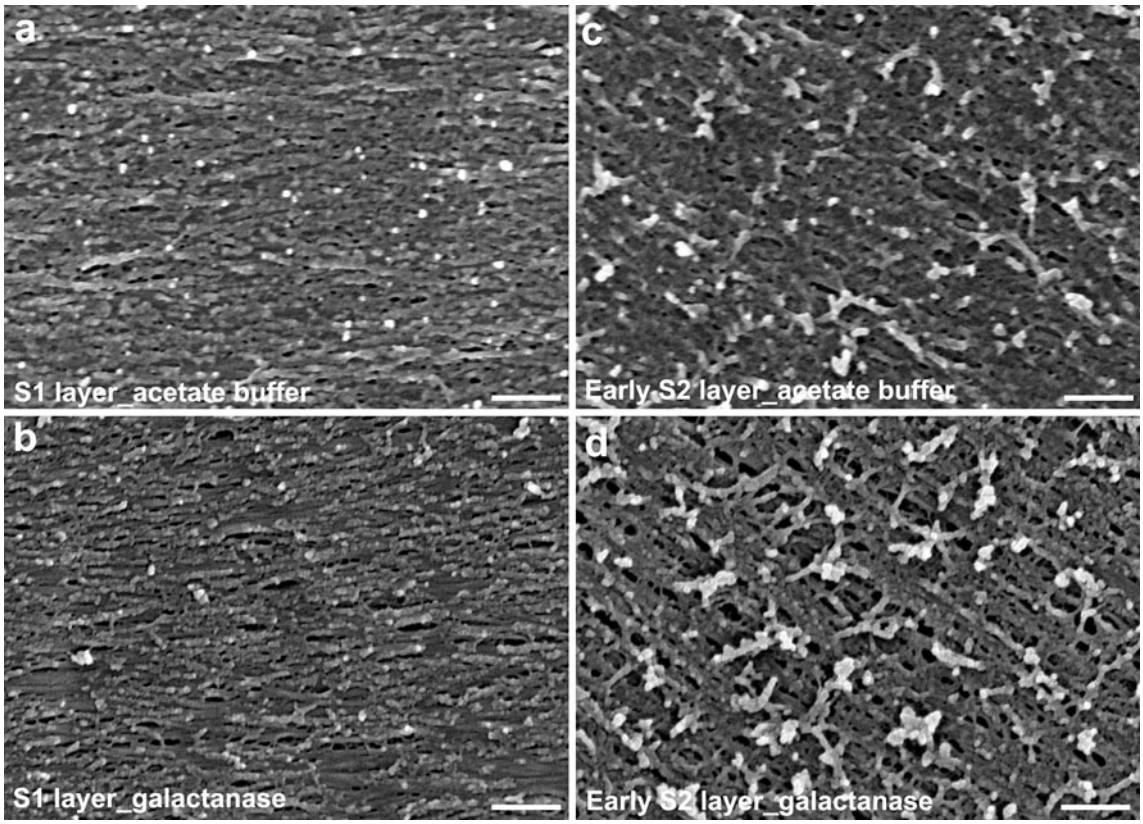

Fig. 7 The innermost surface of compression wood (CW) tracheids after endo-β-1,4-galactanase treatment (**b**, **d**). Amorphous materials decreased significantly on the innermost surface of tracheids in the early secondary cell wall formation stage compared to those in the control incubated only with acetate buffer (**a**, **c**), note the appearance of CMF bundles on the innermost surface of tracheids (**b**, **d**). *Bar* 250 nm

β-mannanase treatment, and CMF bundles were not exposed on the innermost surface (Fig. 2h), whereas CW tracheids showed thin CMF bundles on the innermost surface (Fig. 5h) and exhibited different ultrastructural properties compared to those treated with xylanase (Fig. 5d). Delignified mature CW tracheids treated with xylanase revealed a smooth surface on the CMF bundles and compact CMF bundle structures (Fig. 6a), whereas delignified CW tracheids treated with β-mannanase (Fig. 6b) showed an uneven surface and more loose structure of the CMF bundles than those treated with xylanase (Fig. 6a). This result indicates that the uneven surface of CMF bundles caused by β-mannanase treatment may be related to the presence of xylans. This idea is further supported by the observation that delignified CW tracheids treated with β-mannanase followed by xylanase treatment (Fig. 6c) exhibited a smooth surface and compact structure of the CMF bundle, as in tracheids treated only with xylanase (Fig. 6a). Xylan degradation from the uneven surface of CMF bundles resulted in a more compact CMF bundle structure in mature tracheids than those treated with β-mannanase. These types of ultrastructural properties following the hemicellulase treatments were not observed in NW tracheids, indicating differences in the organization of hemicelluloses in the cell wall between NW and CW tracheids. In addition, delignified mature NW and CW tracheids showed many globular substances on the CMF bundles after the enzyme treatments (Figs. 3, 6). However, the chemical and functional properties of the globular substances are not clearly understood.

In conclusion, the present results suggest that there may be some differences in the ultrastructural organization of hemicelluloses and lignin in CW tracheids and NW tracheids. In our previous immunocytochemical studies, CW tracheids also showed significant differences in hemicellulose distribution in the secondary cell wall, compared to those in NW tracheids (Kim et al. 2010, 2011). Although the roles of cell wall components in CW tracheid formation are not clearly understood, our recent CW tracheid studies, including the present work, suggest that CW tracheids may have different ultrastructural deposition and organization of cell wall components, specifically hemicelluloses and lignin, and that this may be an important factor regulating the CW tracheid architecture which is distinct from that of NW tracheids.

Acknowledgments Jong Sik Kim is grateful for the Research Fellowship for Young Scientists provided by the Japan Society for the Promotion of Science (JSPS).

References

Atalla R (2005) The role of the hemicelluloses in the nanobiology of wood cell walls. A systems theoretic perspective. In: Proceedings of the hemicelluloses workshop 2005. University of Canterbury, Christchurch, pp 37–57

Awano T, Takabe K, Fujita M (2002) Xylan deposition on secondary wall of *Fagus crenata* fiber. Protoplasma 219:106–115

Baird WM, Johnson MA, Parham RA (1974) Development and composition of the warty layer in balsam fir. II. Composition. Wood and Fiber 6:211–222

Côté WA, Day AC (1962) Vestured pits—fine structure and apparent relationship with warts. Tappi 45:906–910

Côté WA Jr, Pickard PA, Timell TE (1967) Studies on compression wood. IV. Fractional extraction and preliminary characterization of polysaccharides in normal and compression wood of Balsam fir. Tappi 50:350–356

Donaldson LA (2001) Lignification and lignin topochemistry—an ultrastructural view. Phytochemistry 57:859–873

Donaldson L (2007) Cellulose microfibril aggregates and their size variation with cell wall type. Wood Sci Technol 41:443–460

Hoffmann GC, Timell TE (1972) Polysaccharides in compression wood of tamarack (*Larix laricina*). 2. Constitution of a galactoglucomannan. Svensk Paperstidn 75:297–298

Iwata T, Indrarti L, Azuma J (1998) Affinity of hemicellulose for cellulose produced by *Acetobacter xylinum*. Cellulose 5:215–218

Kim JS, Awano T, Yoshinaga A, Takabe K (2010) Immunolocalization of β-1-4-galactan and its relationship with lignin distribution in developing compression wood of *Cryptomeria japonica*. Planta 232:109–119

Kim JS, Awano T, Yoshinaga A, Takabe K (2011) Occurrence of xylan and mannan polysaccharides and their spatial relationship with other cell wall components in differentiating compression wood tracheids of *Cryptomeria japonica*. Planta 233:721–735

Nanayakkara B, Manley-Harris M, Suckling ID, Donaldson LA (2009) Quantitative chemical indicators to assess the gradation of compression wood. Holzforschung 63:431–439

Ruel K, Chevalier-Billosta V, Guillemin F, Sierra JB, Joseleau J-P (2006) The wood cell wall at the ultrastructural scale-formation and topochemical organization. Maderas Ciencia y Tecnologiá 8:107–116

Salmén L, Burgert I (2009) Cell wall features with regard to mechanical performance. Holzforschung 63:121–129

Terashima N, Awano T, Takabe K, Yoshida M (2004) Formation of macromolecular lignin in ginko xylem cell walls as observed by field emission scanning electron microscopy. C R Biologie 327: 903–910

Terashima N, Kitano K, Kojima M, Yoshida M, Yamamoto H, Westermark U (2009) Nanostructural assembly of cellulose, hemicellulose, and lignin in the middle layer of secondary wall of ginko tracheid. J Wood Sci 55:409–416

Timell TE (1986) Compression wood in gymnosperms, vol 1. Springer-Verlag, Berlin

Tokoh C, Takabe K, Fujita M, Saiki H (1998) Cellulose synthesized by *Acetobacter xylinum* in the presence of acetyl glucomannan. Cellulose 5:249–261

Tokoh C, Takabe K, Sugiyama J, Fujita M (2002a) Cellulose synthesized by *Acetobacter xylinum* in the presence of plant cell wall polysaccharides. Cellulose 9:65–74

Tokoh C, Takabe K, Sugiyama J, Fujita M (2002b) CP/MAS ^{13}C NMR and electron diffraction study of bacterial cellulose structure affected by cell wall polysaccharides. Cellulose 9:351–360

Uhlin KI, Atalla RH, Thompson NS (1995) Influence of hemicelluloses on the aggregation patterns of bacterial cellulose. Cellulose 2:129–144

Yeh TF, Goldfarb B, Chang HM, Peszlen L, Braun JL, Kadla JF (2005) Comparison of morphological and chemical properties between juvenile wood and compression wood of loblolly pine. Holzforschung 59:669–674

Yeh TF, Braun JL, Goldfarb B, Chang HM, Kadla JF (2006) Morphological and chemical variations between juvenile wood, mature wood, and compression wood of loblolly pine (*Pinus taeda* L.). Holzforschung 60:1–8